Development 135, 599-608 (2008) doi:10.1242/dev.012377

KBP is essential for axonal structure, outgrowth and maintenance in zebrafish, providing insight into the cellular basis of Goldberg-Shprintzen syndrome

David A. Lyons, Stephen G. Naylor, Sara Mercurio, Claudia Dominguez and William S. Talbot*

Mutations in Kif1-binding protein/KIAA1279 (KBP) cause the devastating neurological disorder Goldberg-Shprintzen syndrome (GSS) in humans. The cellular function of KBP and the basis of the symptoms of GSS, however, remain unclear. Here, we report the identification and characterization of a zebrafish *kbp* mutant. We show that *kbp* is required for axonal outgrowth and maintenance. In vivo time-lapse analysis of neuronal development shows that the speed of early axonal outgrowth is reduced in both the peripheral and central nervous systems in *kbp* mutants. Ultrastructural studies reveal that *kbp* mutants have disruption to axonal microtubules during outgrowth. These results together suggest that *kbp* is an important regulator of the microtubule dynamics that drive the forward propulsion of axons. At later stages, we observe that many affected axons degenerate. Ultrastructural analyses at these stages demonstrate mislocalization of axonal mitochondria and a reduction in axonal number in the peripheral, central and enteric nervous systems. We propose that *kbp* is an important regulator of axonal development and that axonal cytoskeletal defects underlie the nervous system defects in GSS.

KEY WORDS: Kif1-binding protein, Axonal outgrowth, Mental retardation, Neurodegeneration, Zebrafish

INTRODUCTION

Axon guidance is fundamental to the establishment of a functional nervous system, and factors that guide axons to their correct targets have been well studied (Maness and Schachner, 2007; Polleux et al., 2007; Zou and Lyuksyutova, 2007). Axons advance forwards when there is a net increase in the polymerization of microtubules at their plus ends, localized within the growth cone (Gordon-Weeks, 2004). In contrast to our understanding of the nature of guidance cues that direct axons to their target, we know comparatively little about the downstream factors that regulate the structure and function of the cytoskeleton during axonal outgrowth, maintenance or disease.

The Stathmin family of phospho-proteins is one of a small number that have been shown to interact with and regulate the dynamics of microtubules (Grenningloh et al., 2004). Stathmin itself can destabilize microtubules (Belmont and Mitchison, 1996), whereas another family member, SCG10, can stabilize microtubules at their plus ends and destabilize them at their minus ends (Manna et al., 2007). Structural microtubule associated proteins (MAPs) can also regulate microtubule dynamics (Baas and Qiang, 2005). Overexpression of the most prominent axonal MAP, tau, compromises the ability of kinesin motor proteins to bind to microtubules (Mandelkow et al., 2003; Stamer et al., 2002), causing a cascade of events that can lead to the severing of microtubules themselves (Baas and Qiang, 2005; Qiang et al., 2006; Yu et al., 2005). Increasing data suggest that defects in microtubule based axonal transport may cause neural degeneration that is symptomatic of many human neurological disorders, including Alzheimer's disease, Parkinson's disease and amyotrophic lateral sclerosis (ALS) (Duncan and Goldstein, 2006). Indeed, the protein products of genes linked to Alzheimer's disease, Parkinson's disease and ALS are all transported along the axon and their mislocalization may even contribute to disease symptoms (Duncan and Goldstein, 2006). These data highlight the importance of microtubule organization and of microtubule based axonal transport during axonal maintenance and disease.

Although genetic and biochemical approaches have provided great insight into the function of kinesin superfamily (Kif) motor proteins during neuronal development and disease (Hirokawa and Takemura, 2005), we are only beginning to understand the function of additional factors that affect their regulation. Biochemical characterization of a novel factor called Kif1-binding protein (KBP) showed that it can bind to the motor domain of the related kinesin motor proteins Kif1B and Kif1C, and in vitro analyses suggested that it may regulate motor protein motility on microtubules (Wozniak et al., 2005). However, further biochemical characterization of this factor is limited, and it is possible that KBP could bind to other related kinesins or indeed to unrelated molecules. Interestingly, homozygous mutations of KBP, also known as KIAA1279, cause a rare but severe neurological disorder, Goldberg-Shprintzen syndrome (GSS), in humans (Brooks et al., 2005). GSS is characterized primarily by neurological symptoms, including mental retardation and disruption to white matter tracts (Fryer, 1998; Goldberg and Shprintzen, 1981; Murphy et al., 2006; Silengo et al., 2003; Tanaka et al., 1993; Yomo et al., 1991). Very little is known about the cellular basis of GSS and in the absence of an animal model that disrupts KBP activity, elucidation of its function during neural development and disease has remained limited.

Here, we present the characterization of a zebrafish kinesin *kbp* mutant. We show that *kbp* mutant axons grow at reduced speeds and that many axons undergo degeneration at later stages. Ultrastructural analyses demonstrate disruption to axonal microtubules at early stages and further disruption to microtubules and mislocalization of axonal mitochondria at later stages. Based on these data, we propose that KBP is an important regulator of the axonal cytoskeleton that affects the speed of

Department of Developmental Biology, Stanford University School of Medicine, Stanford, CA 94305, USA.

*Author for correspondence (e-mail: talbot@cmgm.stanford.edu)

Accepted 12 November 2007

axonal outgrowth and the maintenance of axons. These data provide insight into the function of KBP during neural development and support the growing body of evidence that disruption to the axonal cytoskeleton can contribute to human disease.

MATERIALS AND METHODS

Fish stocks

The *kbp*^{st23} mutation was identified in an ENU-based screen for mutations that disrupted myelinated axons (Pogoda et al., 2006). Tg(Foxd3:gfp)[17] fish (Gilmour et al., 2002) were kindly provided by Darren Gilmour, and Tg(HuC:kaede)^{rw0130a} fish (Sato et al., 2006) by Hitoshi Okamoto.

Positional cloning and molecular analyses of *kbp*

The *st23* mutation was mapped by bulked segregant analyses with SSLPs by standard methods (Talbot and Schier, 1999). Initial mapping placed the *st23* mutation between markers z47593 (one recombinant out of 688 meioses) and z67865 (42/688) on linkage group 13. To generate additional markers for high-resolution mapping, we consulted the zebrafish genome assembly. Among the markers that failed to recombine with the mutation was one associated with the zebrafish ortholog of *kbp*. We sequenced the *kbp* gene from wild-type genomic DNA, confirming the gene structure predicted by the Sanger Institute. Sequencing of mutant genomic DNA identified a GT to AT mutation that disrupted the splice donor at the beginning of intron 5. The full-length *kbp* coding sequence was submitted to GenBank (Accession number EU234534).

To determine whether *kbp* mRNA was present in *kbp*^{st23} mutants, RNA was extracted from larvae at 7 days post fertilization (dpf), which were sorted from a *kbp*^{st23}/+, Tg(Foxd3:gfp) intercross. For some experiments, RNA was extracted from individual genotyped (see below) embryos. RT-PCR was carried out on cDNA with primers flanking the lesion site, one in exon 5, 5′-ATGGAGGCTCGTCATTGTTT-3′ and one in exon 6, 5′-GCATCTTGCAACAAATTAAGG-3′. RT-PCRs were carried out with a 2.5-minute extension for 44 cycles. RT-PCR was also carried out using primers spanning exons 4-6, one in exon 4, 5′-CGCACAC-GCTGTATTACCTG-3′ and one in exon 6, 5′-GATCCAGCATCTG-GCAATTT-3′. These RT-PCRs were carried out with a 1-minute extension for 30 cycles.

Genotyping

Two DCAPS assays were used to score for the *kbp*^{st23} mutation. PCR was carried out with 5′-CTCAGAGGCAGCTGCCAAACTAA-3′ and 5′-ACGACACTGTTTCAGAAGAA-3′, and PCR products digested with the restriction enzyme *Dde*I, yielding a smaller fragment from the wild-type allele. In more recent experiments, PCR was carried out with a second set of primers, 5′-AAAACGACCAACTGTGCCTA-3′ and 5′-ACAGTCAA-ACACCAGATCGAAAGTCA-3′ and digested with *Mae*III, yielding a smaller fragment from the wild-type allele.

kbp morpholino

Embryos were injected at the one-cell stage with 2.4 ng of a morpholino antisense oligonucleotide spanning the end of exon 1 and the beginning of intron 1 of zebrafish *kbp* (5′-GTTAGTGTGTATTTACCCGGACATG-3′), obtained from Gene Tools.

In situ hybridization

To synthesize *kbp* riboprobes, a 1815 bp region covering exons 1-7 was PCR amplified from cDNA made from zebrafish at 72 hours post-fertilization (hpf), with the following primers: F, 5′-TGGCTGCCAACACAGTATCG-3′ and R, 5′-GCTCGGTTTCTACAGCGTTC-3′. The PCR product was cloned into pCR II-TOPO vector (Invitrogen) and sequenced. This construct was linearized by *Xba*I and transcribed with SP6 for antisense and linearized with *Bam*HI and transcribed with T7 for sense.

Immunohistochemistry

Anti-acetylated tubulin (Sigma) was used at a dilution of 1:1000, anti-HuC/D (Molecular probes) at 1:500 and secondary antibodies conjugated to either Alexa488 or Alexa568 (Molecular probes) at 1:2000. Images were taken on a Zeiss LSM confocal microscope.

Transplantation

To generate chimeric embryos, we transplanted cells at the blastula stage from wild-type donor embryos labeled with 1% Texas Red dextran (Molecular Probes) into *kbp*^{st23} mutant hosts. Live chimeras were imaged at 80 hpf, and genotypes were determined by PCR as described above.

Time-lapse microscopy and analyses

Embryos were imbedded in 1.5% low melting point agarose in embryo medium with Tricaine and imaged on a Zeiss LSM confocal microscope. All time-lapse recordings were carried out at 28.5°C with an interval of 5 minutes. Analyses of time-lapse data were carried out using ImageJ.

Axonal mitochondrial and synaptic vesicle protein labeling

To co-label axons and mitochondria single cells were injected with 1% Oregon Green Dextran (Molecular Probes) and 200 ng/μl mito:mCherry mRNA at the 32-256 cell stage. Embryos were screened at 48 hpf and those with labeled PLL or reticulospinal neurons were selected and imaged.

To co-label axons and synaptophysin, embryos were injected at the one cell stage with 25 pg of syn:GFP-DSR plasmid DNA (Meyer and Smith, 2006). Embryos were screened at 96 hpf and those with suitably labeled neurons were imaged.

Cartilage staining

Alcian Blue (0.1% in 0.37% HCl, 70% ethanol) was used to label cartilage according to standard protocols (Schilling et al., 1996).

Transmission electron microscopy

Embryos were fixed for TEM in modified Karnovsky's solution (2% glutaraldehyde + 4% paraformaldehyde in 0.1 M sodium cacodylate buffer), post fixed in 2% osmium tetroxide in 0.1 M imidazole and 0.1 M sodium cacodylate, stained en bloc in saturated uranyl acetate, and dehydrated into 100% acetone. All of these steps were accelerated by a microwave stimulation regime using the PELCO 3470 Multirange Laboratory Microwave System (Pelco) and kept at 15°C in a cooled water bath using the PELCO Steady Temp throughout. Following dehydration, embryos were embedded in Epon, and stained and imaged as described previously (Pogoda et al., 2006).

RESULTS

Abnormal axonal development in *kbp*^{st23} mutants

In a screen for zebrafish mutants with abnormalities in myelinated axons, we uncovered a mutation, *kbp*^{st23}, in a gene that is required for the development of peripheral axons in the larva (Pogoda et al., 2006). Analyses using the transgene Tg(HuC:kaede) (Sato et al., 2006) showed that by 28 hpf, migrating growth cones of wild-type animals have reached somite 11-12 (Fig. 1A), whereas those in *kbp*^{st23} mutants have usually only navigated as far as somite 9-10 (Fig. 1B). The most advanced wild-type growth cones have a highly branched morphology (Fig. 1A), indicative of active migration, whereas those in *kbp*^{st23} mutants do not exhibit such an elaborate morphology (Fig. 1B). We also observed defects during axonal outgrowth in the CNS. Axons of reticulospinal neurons are among the first to initiate outgrowth in the zebrafish CNS, and many of these migrate from their origin in the hindbrain to the posterior end of the spinal cord. We observed that by 30 hpf some reticulospinal axons had advanced along the ventral spinal cord to an anteroposterior position corresponding to the level of somite 18-20 (Fig. 1C). By contrast, those in *kbp*^{st23} mutants lagged significantly behind, having only reached a position corresponding to somites 14-16 (Fig. 1D). The overall number and distribution of neuronal cell bodies, however, was normal in the CNS, PNS and ENS of *kbp*^{st23} mutants at all stages examined (Fig. 1E,F and data not shown). Furthermore, homozygous *kbp*^{st23} mutants are morphologically indistinguishable from their siblings (Fig. 1G,H) through at least 10 dpf and survive for about 12 dpf, long after axonal defects emerge. These data show that *kbp*^{st23} specifically affects axonal development.

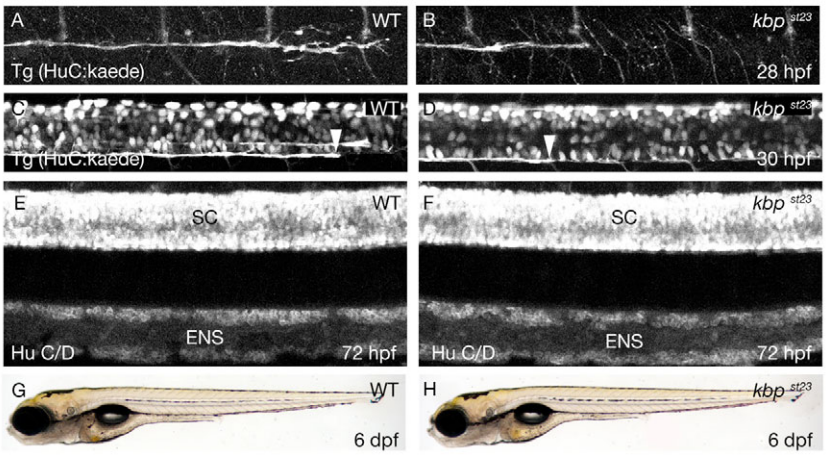

Fig. 1. The *kbp*^{st23} mutation disrupts axonal development. (**A**,**B**) Lateral views of PLLn axons in live embryos bearing the Tg(HuC:kaede) transgene at 28 hpf. Axons of the wild type (A) have advanced further posterior than those in the *kbp*^{st23} mutant (B). The images show the segment of the nerve corresponding to about somites 6-12. Anterior is towards the left and dorsal towards the top. (**C**,**D**) Lateral views of spinal cord axons in live embryos bearing the Tg(HuC:kaede) transgene at 30 hpf. The arrowheads indicate the posterior-most axons in the ventral spinal cord tract in the wild type (C) and the *kbp*^{st23} mutant (D). The images show the segment of the spinal cord corresponding to about somites 14-20. Anterior is towards the left and dorsal towards the top. (**E**,**F**) Lateral views of embryos at 72 hpf showing neurons labeled with anti-HuC/D in the spinal cord (SC) and enteric nervous system (ENS) of a wild-type (E) and *kbp*^{st23} mutant (F). There are no discernable differences in neuronal organization between *kbp*^{st23} mutants and siblings. (**G**,**H**) Lateral views of live larvae at 6 dpf show no obvious morphological differences between wild-type (G) and *kbp*^{st23} mutant (H) larvae. The genotypes of all specimens were determined after photography (see Materials and methods).

The *kbp*^{st23} mutation disrupts the zebrafish *kbp* gene

Through high-resolution mapping and positional cloning, we discovered that the *kbp*^{st23} mutation disrupts the zebrafish ortholog of human kinesin Kif1-binding protein (KBP)/KIAA1279 (Fig. 2), which is 54% identical and 73% similar to its human counterpart. The zebrafish gene comprises seven exons (Fig. 2A), and sequencing showed that the *kbp*^{st23} mutation alters the splice donor (GT>AT) after exon 5 (Fig. 2). High-resolution mapping shows that this lesion co-segregates with the mutation: all mutants tested (n=50) were homozygous for the lesion**.** RT-PCR showed that *kbp* is expressed maternally and becomes reduced during gastrulation, but is expressed at higher levels again at later stages (data not shown). In situ hybridization showed primarily neuronal expression of *kbp* at later stages, in both the CNS and PNS (Fig. 2D). RT-PCR showed that there is no detectable wild-type *kbp* mRNA in *kbp*^{st23} mutants, but we did identify four aberrant *kbp* transcripts in the mutants (Fig. 2B). The most prominent of these transcripts, mut1,

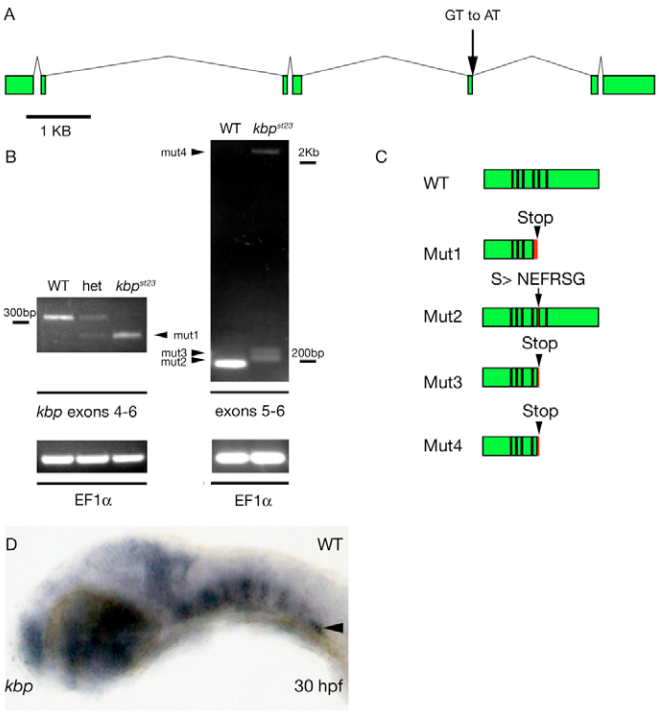

Fig. 2. The *kbp*^{st23} mutation disrupts the zebrafish *kbp* gene. (**A**) Genomic structure of zebrafish *kbp*. Green boxes indicate coding sequences of *kbp* exons. Scale bar is 1 kb. The splice donor disrupted by the *st23* lesion is indicated by the arrow. (**B**) RT-PCR detects aberrant *kbp* transcripts in *kbp*^{st23} mutant larvae. Gel on left shows RT-PCR products generated with primers from exons 4 and 6 on RNA isolated from homozygous wild-type, heterozygous and *kbp*^{st23} mutant embryos. The lower mutant band, mut1 (arrowhead), reflects the deletion of exon 5 in the spliced mutant transcript. Gel on the right shows RT-PCR products generated with primers from exons 5 and 6 from RNA isolated from a mixture of larvae with wild-type phenotypes (i.e. homozygous wild type and heterozygous) and a group of *kbp*^{st23} mutant larvae. *kbp*^{st23} mutants have three weakly expressed transcripts (arrowheads) that result from aberrant splicing at the exon 5-6 junction. Below are loading controls showing that *EF1α* mRNA is robustly detected in all samples. (**C**) Schematic depicting the structure of the wild-type KBP protein and the abnormal products predicted to result from the four mutant *kbp* mRNAs. Red indicates regions encoded by intronic sequence and arrowheads indicate the positions of the premature stop codons predicted to truncate the proteins encoded by mutant mRNAs. Black lines separate coding sequences derived from different exons. (**D**) Lateral view of a wild-type embryo at 30 hpf showing *kbp* mRNA expression. Anterior is towards the left and dorsal is towards the top. The arrowhead indicates *kbp* expression in the posterior lateral line ganglion.

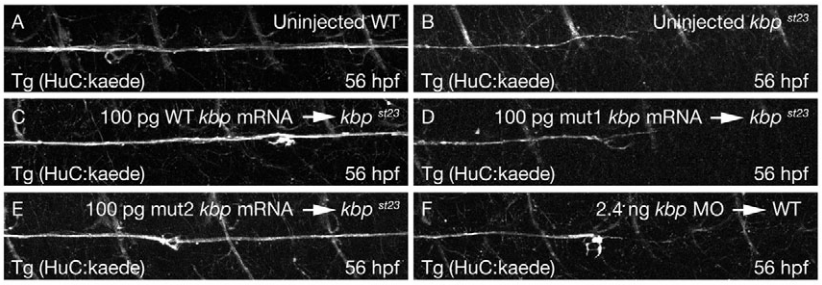

Fig. 3. KBP is required for axonal development. Lateral views of PLLn axons in live embryos bearing the Tg(HuC:kaede) transgene at 56 hpf. The images show the segment of the nerve corresponding to about somites 10-16. Axons of the wild type (**A**) have advanced further posterior than those in the *kbp*^{st23} mutant (**B**). Axonal outgrowth is rescued in *kbp*^{st23} mutants injected with full-length wild-type *kbp* mRNA (**C**) and the mut2 *kbp* mRNA (**E**), but not in *kbp*^{st23} mutants injected with the mut1 *kbp* mRNA (**D**). Wild-type embryos injected with 2.4 ng of *kbp* morpholino (**F**) resemble *kbp*^{st23} mutants. In all images, anterior is towards the left and dorsal is towards the top.

lacks exon 5, so that exon 4 is spliced to exon 6. This aberrant transcript encodes a truncated KBP protein (Fig. 2B,C). Using primers in exons 5 and 6, we detected lower levels of three additional transcripts. One of these, mut4, retains the entire fifth intron, which contains many in frame stop codons, also leading to a truncated protein (Fig. 2C). The other two transcripts are spliced from two different GT di-nucleotides near the beginning of the fifth intron that can apparently serve as splice donors in the absence of the wild-type donor sequence. The larger of these aberrantly spliced transcripts, mut3, encodes the same truncated product as the unspliced mut4 RNA (Fig. 2C): it contains intronic sequence encoding two premature stop codons and splices out of frame to exon 6. The smaller aberrantly spliced transcript, mut2, splices in-frame to exon 6, with the inclusion of intronic sequence that replaces serine 302 of the wild-type protein with a six amino acid sequence (NEFRSG) (Fig. 2C).

To assess the possible functions of the different forms of *kbp*^{st23} mRNA, we injected synthetic *kbp* mRNA into *kbp*^{st23} mutants. Injection of full-length wild-type *kbp* mRNA completely restored normal axonal outgrowth, in the PNS and the CNS (Fig. 3C, Table 1 and data not shown). Injection of the most abundant form of *kbp*^{st23} mRNA (mut1, lacking exon 5), however, completely failed to rescue axonal outgrowth (Fig. 3D and Table 1). By contrast, injection of mut2 mRNA, which encodes the six amino acid substitution, was capable of restoring normal axonal development in *kbp*^{st23} mutants (Fig. 3E and Table 1), showing that the Mut2 protein is functional. The mut2 *kbp*^{st23} mRNA, however, constitutes only a few percent of the *kbp*^{st23} RNA species present in the mutant, as only one out of more than 40 *kbp* cDNA clones recovered from mutant RNA represented this splice form.

Table 1. Summary of functional activity of wild-type and mutant *kbp* mRNA

	Embryos	*kbp*^{st23}	*kbp*^{st23} with normal axons
Uninjected	68	21	0 (0%)
100 pg wild-type *kbp* RNA	71	19	19 (100%)
100 pg mut1 *kbp* RNA	61	21	0 (0%)
100 pg mut2 *kbp* RNA	64	15	15 (100%)

As an additional and independent means to knock down KBP function, we used a morpholino antisense oligonucleotide directed against the exon 1-intron 1 splice junction of *kbp*. Injection of this morpholino produced an almost identical phenotype to that of the *kbp*^{st23} mutant in 35 out of 37 injected embryos, with axonal defects in both the PNS and CNS but no observable effects on general development (Fig. 3F and data not shown). Collectively, these data show that the *kbp*^{st23} mutation disrupts the zebrafish *kbp* gene and represents a strong loss of function of KBP. As mutations in KBP cause Goldberg-Shprintzen syndrome (GSS) in humans (Brooks et al., 2005), the *kbp*^{st23} mutation provides a new animal model of GSS.

KBP is required autonomously in neurons for axonal outgrowth

To test whether KBP was required cell autonomously in neurons for normal axonal development, we created genetic chimeras by transplanting fluorescently labeled wild-type cells into *kbp*^{st23} mutant animals at blastula stages. In five such chimeras, at 80 hpf, we saw wild-type reticulospinal neurons with axons that extended

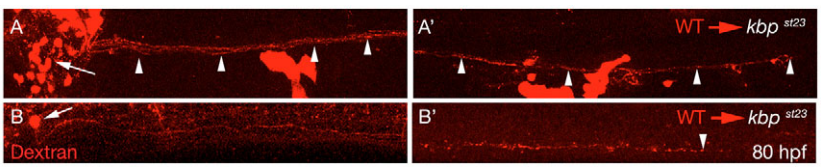

Fig. 4. *kbp* is required autonomously in neurons for axonal outgrowth. (**A**,**A'**) Lateral views of a chimeric larva generated by transplantation of dextran labeled wild-type cells (red) into a *kbp*^{st23} mutant. Wild-type neurons in the PLLg (arrow, A) extend axons along the entire length of the PLL (A'). Arrowheads point to extended PLLn axons and the rightmost arrowhead in A' represents an axon innervating the most posterior neuromast near the tip of the tail. (**B**,**B'**) Lateral views of a chimeric larva generated by transplantation of dextran-labeled wild-type cells (red) into a *kbp*^{st23} mutant. A single wild-type reticulospinal neuron in the hindbrain (arrow, B) extends an axon along the entire length of the spinal cord (B'). Arrowhead indicates the end of the axon near the tip of the tail.

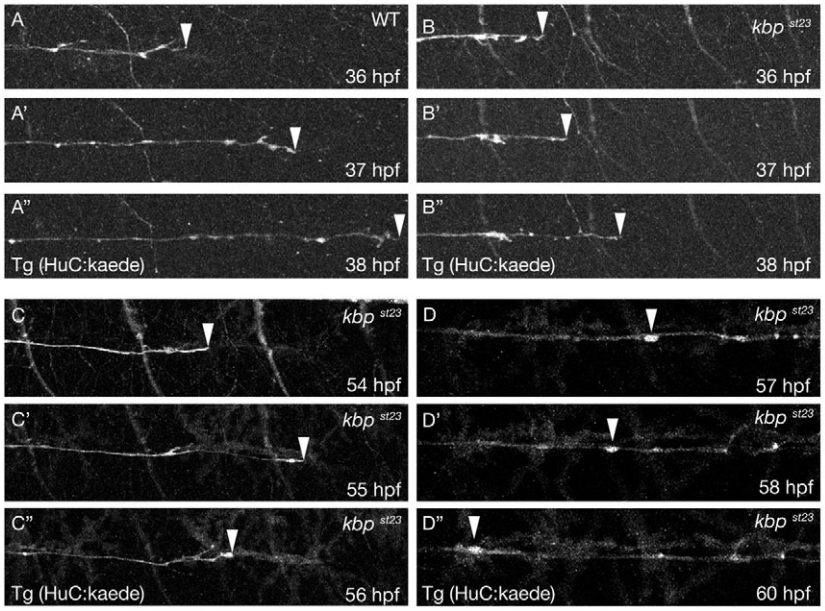

Fig. 5. KBP is required to maintain the speed of axonal outgrowth in the PNS. (**A-A″**) Lateral views from a time-lapse series of a wild-type embryo with PLLn axons labeled by the Tg(HuC:kaede) transgene at 36 (A), 37 (A′) and 38 hpf (A″). Anterior is towards the left and dorsal is towards the top. The arrowheads indicate the posteriormost axons. (**B-B″**) Lateral views from a time-lapse series of a *kbp*^{st23} mutant embryo with PLLn axons labeled by the Tg(HuC:kaede) transgene at 36 (B), 37 (B′) and 38 hpf (B″). Anterior is towards the left and dorsal is towards the top. The arrowheads indicate the posteriormost axons. (**C-C″**) Lateral views from a time-lapse series of a *kbp*^{st23} mutant embryo with PLLn axons labeled by the Tg(HuC:kaede) transgene at 54 (C), 55 (C′) and 56 hpf (C″). Anterior is towards the left and dorsal is towards the top. The arrowheads indicate the posteriormost axons. (**D-D″**) Lateral views from a time-lapse series of a *kbp*^{st23} mutant embryo with PLLn axons labeled by the Tg(HuC:kaede) transgene at 57 (D), 58 (D′) and 60 hpf (D″). Anterior is towards the left and dorsal is towards the top. Arrowheads indicate an axonal swelling that moves backwards along the nerve.

down the entire length of the spinal cord (Fig. 4B,B′). In two additional cases, we saw wild-type PLL neurons with axons that extended along the entire length of the lateral line (Fig. 4A,A′). We have never seen reticulospinal or PLL neurons with axons that extend along the entire length of their respective tissues in the *kbp*^{st23} mutant. These data show that *kbp* is required autonomously in neurons for axonal outgrowth.

kbp is required to maintain axonal outgrowth

Time-lapse imaging of *kbp*^{st23} mutant PLLn axons labeled with Tg(HuC:kaede) revealed a range of aberrant behaviors. Many axons advanced at very slow rates compared with wild-type siblings (Fig. 5A,B; see Movies 1 and 2 in the supplementary material). We also observed that *kbp*^{st23} mutant PLLn axons can undergo consecutive periods of forward growth and retraction (Fig. 5C-C″) and thus fail to advance forward, despite exhibiting dynamic activity (see Movie 3 in the supplementary material). This behavior was not observed in wild type. We also observed disruption to the behavior of growing axons in the *kbp*^{st23} mutant CNS. Reticulospinal axons grow along relatively straight tracts in the ventral spinal cord and exhibit little exploratory pathfinding behavior (see also Jontes et al., 2000), allowing straightforward measurement of their outgrowth speed. We saw that although wild-type growth cones move at an average speed of 1.8±0.5 μm/minute (n=21) between 24 and 48 hpf (see Fig. S1A-A″ and Movie 1 in the supplementary material), those of the *kbp*^{st23} mutant travel much more slowly (see Fig. S1B-B″ and Movie 2 in the supplementary material), at a speed of 1.0±0.2 μm/minute (n=33). Thus, our time-lapse analyses show that *kbp* is required to regulate the dynamics of axonal outgrowth in the PNS and CNS.

kbp is required for axonal maintenance

Axons of the *kbp*^{st23} mutant PLLn are typically truncated at the level of somites 6-10 by 5 dpf, but many grow significantly further than this at earlier stages. We performed additional time-lapse experiments between 2 and 3 dpf to look for evidence of axonal degeneration or retraction. We observed net backwards movement of axons in *kbp*^{st23} mutants and noted the periodic formation and backwards movement of punctate axonal swellings in the *kbp*^{st23} mutant PLLn (Fig. 5D-D″ and Movie 3 in the supplementary material). We did not observe axonal swellings such as those in wild type. Axonal swellings are commonly associated with axonal degeneration (Coleman, 2005). Furthermore, we noticed that the PLLn became thinner over time and occasionally noticed fragmentation of axons, also indicative of degeneration. These data suggest that *kbp*^{st23} mutant axons degenerate and that *kbp* is required for the longer-term maintenance of axons in addition to outgrowth.

As previous studies have suggested that KBP may associate with mitochondria (Wozniak et al., 2005) we assessed whether mitochondrial localization was disrupted in *kbp*^{st23} mutant axons. We saw a reduction in the intensity of mito:mCherry labeling in individual *kbp*^{st23} mutant axons compared with wild type, (Fig. 6A-D), but the small size of axonal mitochondria precluded quantitative analysis of mitochondrial distribution and dynamics at the light microscopy level. We did not see any overt defects in the localization of the synaptic vesicle protein marker, synaptophysin:GFP (Meyer and Smith, 2006) in *kbp*^{st23} mutant axons (Fig. 6E,F).

kbp is required for microtubule organization and the localization of axonal cargo

To better understand the cellular basis of *kbp*^{st23} mutant axonal defects, we examined their ultrastructure by transmission electron microscopy (TEM). Close examination of *kbp*^{st23} mutant axons in the PLLn during early stages of outgrowth revealed disorganization of axonal microtubules: in the wild type at 30 hpf, most microtubules are oriented along the long axis of the axon, whereas the microtubules are present in many different orientations in *kbp*^{st23} mutant axons (Fig. 7A,B). We did not observe any differences in the number of axonal mitochondria between wild type and *kbp*^{st23} mutants at these early stages, suggesting that the primary defect in *kbp*^{st23} mutants is disorganization of the axonal cytoskeleton. Examination at later stages demonstrated a decrease in axon number in the *kbp*^{st23} mutant PLLn and dark axonal discoloration (Fig. 7E,F), both of which provide additional evidence of axonal degeneration. In addition, we saw continued disruption to axonal microtubules (Fig. 7C,D) and now also a clear reduction in the number of mitochondria within axons (Fig. 7E,F). At 50 hpf, at somite levels 1, 6 and 12 we counted an average of 64, 48 and 32

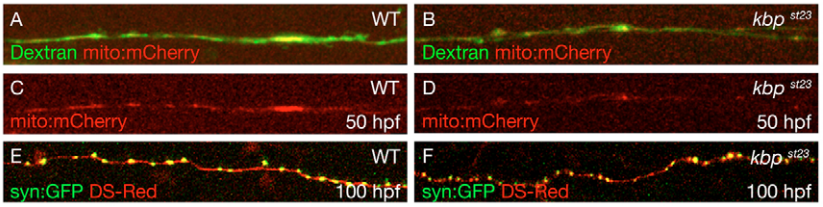

Fig. 6. Localization of mitochondria and synaptic vesicle protein in *kbp*^{st23} mutant axons. (**A-D**) Lateral views of single axons at 50 hpf labeled with Oregon Green Dextran (green) and mitochondria labeled with mito:mCherry mRNA (red) in wild-type (A,C) and *kbp*^{st23} mutant (B,D) embryos. (**E**,**F**) Lateral views of single axons at 100 hpf labeled with DSRed (red) and synaptophysin labeled with syn:GFP (green) in wild-type (E) and *kbp*^{st23} mutant (F) embryos.

axons in the wild-type PLLn, compared with 40, 26 and 7 in the *kbp*^{st23} mutant. Of these 24, 27 and 17% contained a mitochondrion in wild type, compared with 11, 12 and 9% in the *kbp*^{st23} mutant.

We also occasionally observed aberrant accumulations of synaptic vesicles in *kbp*^{st23} mutant axons (Fig. 7C,D), which we never saw in wild type. These results show that *kbp* is required for organization of axonal microtubules, the localization of mitochondria and synaptic vesicles, and the maintenance of axons.

Ultrastructural examination of reticulospinal neurons at 30 hpf proved difficult as these axons do not have distinct morphological features that allow their unambiguous identification among the many other axons in the spinal cord. By 50 hpf, however, we documented a marked reduction in the number of large diameter reticulospinal axons in the ventral spinal cord of *kbp*^{st23} mutants (Fig. 8A,B). We counted an average of 20±2 axons with a diameter greater than 0.75 μm in wild-type animals, compared with an average of only 9±1 axons of that size in the *kbp*^{st23} mutant. As in the PNS, in the wild-type CNS most microtubules are oriented along the long axis of the axon, whereas the microtubules are present in many different orientations in large diameter *kbp*^{st23} mutant axons (Fig. 8A-D). By 72 hpf, we saw further defects in the *kbp*^{st23} mutant CNS. The number of large-diameter axons was still reduced (WT average of 32±1 axons larger than 0.75 μm compared with 15±4 in the *kbp*^{st23} mutant), and most of those that were present in the mutant remained unmyelinated (Fig. 8E,F). In the wild type, more than two-thirds (22 of 32) of axons of greater than 0.75 μm were myelinated, compared with only 40% (6 out of 15) in the *kbp*^{st23} mutant. As at earlier stages, disorganization of the axonal cytoskeleton was also evident at 72 hpf (Fig. 8E,F). In addition, we saw swollen vacuolated mitochondria in *kbp* mutant axons in the CNS and a dark discoloration of some axons, also providing evidence of axonal degeneration in the CNS (McHale et al., 1995). At later stages, we continued to note a reduction in the number of large-diameter axons and hypomyelination in the *kbp*^{st23} mutant (Fig. 8G-I). These data indicate that *kbp* is required for organization of axonal microtubules, and axonal outgrowth and maintenance in the CNS.

kbp is required for axonal development in the enteric nervous system

Histological examination of individuals with GSS has documented variable degrees of aganglionic megacolon, i.e. loss of enteric neurons (Brooks et al., 1999; Murphy et al., 2006; Ohnuma et al.,

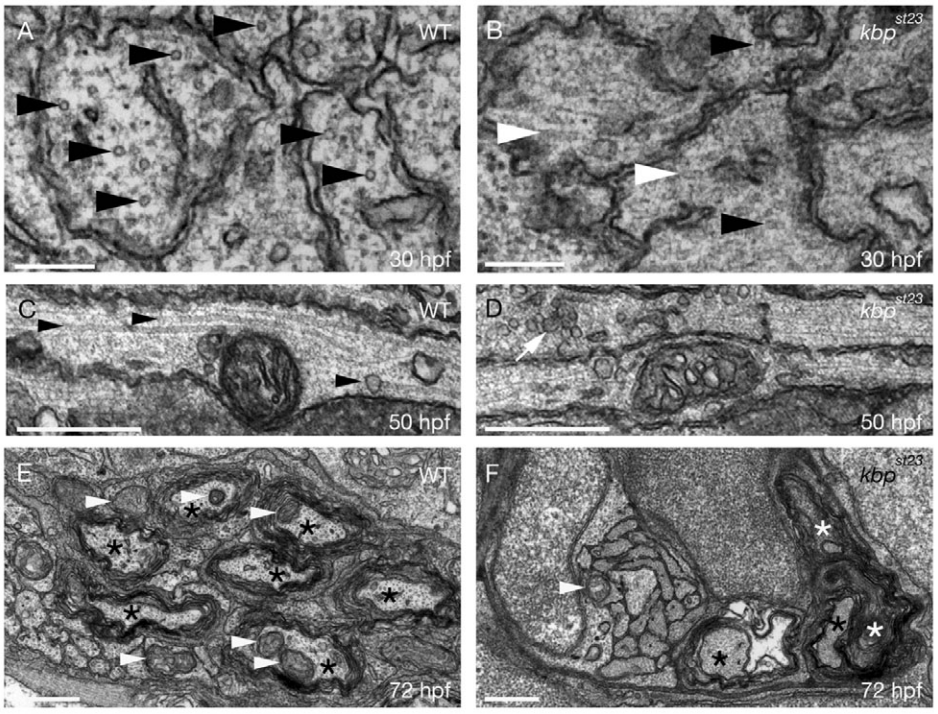

Fig. 7. KBP is required for microtubule organization, localization of axonal mitochondria and synaptic vesicles, and axonal maintenance in the PNS. (**A**,**B**) TEM images of transverse sections through the PLLn at 30 hpf shows more organized microtubules (black arrowheads) in wild-type (A) axons than in *kbp*^{st23} mutant (B) axons and disorganized microtubules (white arrowheads) in *kbp*^{st23} mutant (B) axons. Scale bars: 200 nm. (**C**,**D**) TEM images of longitudinal sections through the PLLn at 50 hpf show more profiles of properly oriented microtubules (arrowheads) running parallel to the long axis of the axon in wild type (C) than in the *kbp*^{st23} mutant (D). White arrow indicates an accumulation of synaptic vesicles in a *kbp*^{st23} mutant axon. Scale bars: 0.5 μm. (**E**,**F**) TEM images of transverse sections through the PLLn at 72 hpf show more myelinated axons (black asterisks) and mitochondria within axons (white arrowheads) in the wild type (E) than in the *kbp*^{st23} mutant. White asterisks in F indicate myelinated axons undergoing degeneration. Scale bars: 0.5 μm.

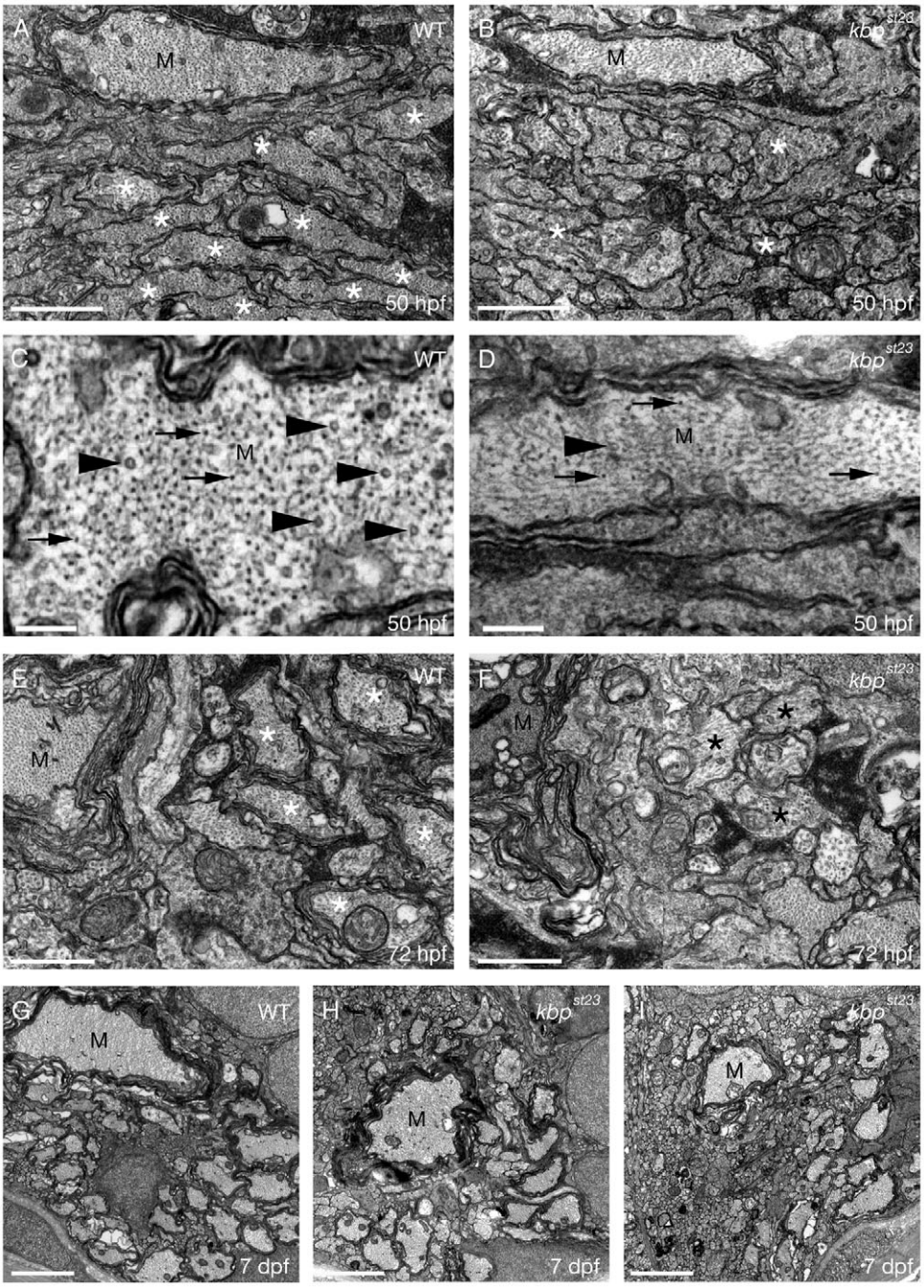

Fig. 8. KBP is required for axonal growth, cytoskeletal organization and myelination in the CNS. (**A**,**B**) TEM images of transverse sections through the ventral spinal cord of a wild type (A) and *kbp*^{st23} mutant (B) at 50 hpf. Axons with a diameter greater than 0.75 μm are indicated by a white asterisk. There are fewer large-diameter axons in the *kbp*^{st23} mutant. Cytoskeletal disorganization is apparent in the large Mauthner axon (M) in the *kbp*^{st23} mutant compared with wild type. Scale bars: 0.75 μm. (**C**,**D**) TEM images of transverse sections through the ventral spinal cord show high magnification views of the Mauthner axon (M) in a wild type (C) and *kbp*^{st23} mutant (D) at 50 hpf. There are more properly oriented microtubules (e.g. arrowheads) and neurofilaments (e.g. arrows) in the wild type than in the *kbp*^{st23} mutant (D) Mauthner axon. Scale bars: 200 nm. (**E**,**F**) TEM images of transverse sections through the ventral spinal cord show that there are more myelinated axons (white asterisks) in wild type (E) than in the *kbp*^{st23} mutant (F) at 72 hpf. Examples of large diameter *kbp*^{st23} mutant axons with a disorganized cytoskeleton are indicated by black asterisks. Scale bars: 0.75 μm. (**G-I**) TEM images of transverse sections through the ventral spinal cord show that there are more large-diameter myelinated axons in the wild type (G) compared with *kbp*^{st23} mutants (H,I) at 7 dpf. Scale bars: 2 μm.

1997; Silengo et al., 2003). Analysis of the neuronal marker HuC/D showed that overt neuronal differentiation is normal in the *kbp*^{st23} mutant ENS until at least 10 dpf (Fig. 9A,B). Examination of the ultrastructure of the enteric nervous system in the *kbp*^{st23} mutant, however, showed that *kbp*^{st23} mutants have a greatly reduced number of axons in the ENS at 7 dpf (wild-type average of 218±42 compared with *kbp*^{st23} average of 97±15). Many of those axons present in the *kbp*^{st23} mutant ENS had disorganized microtubules and abnormal accumulations of axonal synaptic vesicles (Fig. 9C,D). These data show that *kbp* is important for axonal development in the ENS in addition to the PNS and CNS, but that the early differentiation of neural crest-derived neurons is normal. Whereas individuals with GSS also develop craniofacial abnormalities, early development of craniofacial cartilages and other derivatives of the neural crest, such as pigment cells and Schwann cell precursors, are also normal in *kbp*^{st23} mutants (Fig. 9E,F; Fig. 1C,D) (Pogoda et al., 2006).

DISCUSSION

Starting with a genetic screen to isolate mutants that disrupt the development of myelinated axons, we identified a mutation in the gene encoding zebrafish Kif1-binding protein (KBP). Our analyses show that *kbp* is required for axonal outgrowth in the PNS and CNS and for the maintenance of axons at later stages. Time-lapse analyses and ultrastructural studies show that axon outgrowth is slower in *kbp* mutants compared with wild type and that slow outgrowth coincides with disruption to axonal microtubules. At later stages, some axons degenerate, coincident with additional disruption of microtubules

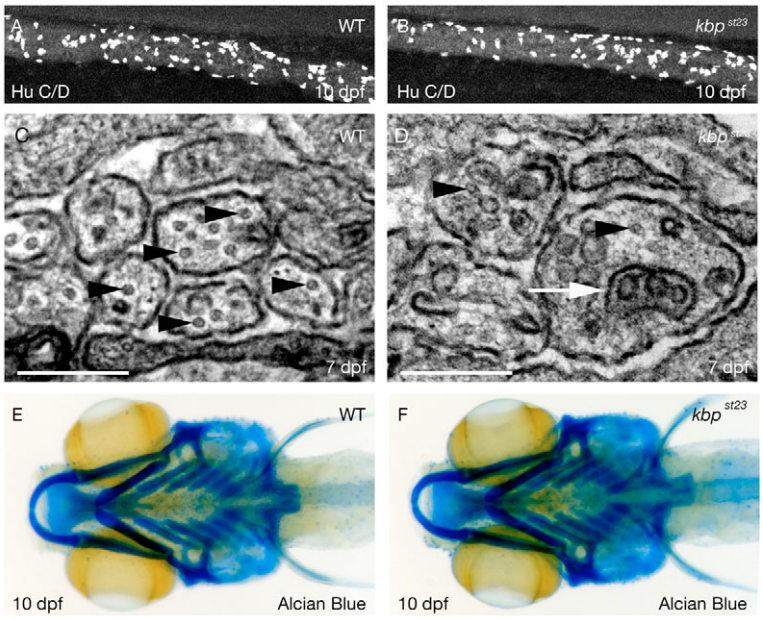

Fig. 9. KBP is required for ENS axonal development, but not for head patterning. (**A**,**B**) Lateral views of larvae at 10 dpf showing neurons labeled with anti HuC/D in the posterior hindgut of the enteric nervous system in a WT (A) and *kbp*^{st23} mutant (B). There were no discernable differences in neuronal organization between *kbp*^{st23} mutants and siblings. (**C**,**D**) TEM images of transverse sections through the enteric nervous system at 7 dpf shows a group of small axons with organized microtubules (arrowheads) in wild type (C) and more disorganized axons with accumulations of vesicles (arrow) in the mutant (D). Scale bars: 200 nm. (**E**,**F**) Ventral views of larvae at 10 dpf showing head cartilages labeled by Alcian Blue in a wild type (E) and *kbp*^{st23} mutant (F). There were no discernable differences in the organization of the head skeleton between *kbp*^{st23} mutants and siblings.

and the mislocalization of axonal mitochondria and synaptic vesicles. Our examination also revealed a reduction in myelination in *kbp* mutants. This is likely to be a secondary consequence of axonal defects, but we do not rule out a potential additional role for *kbp* in glial cells. Our analysis shows that *kbp* is required for microtubule organization, axonal outgrowth, the localization of axonal cargo and the maintenance of axons. We suggest that disruption of these processes may underlie the symptoms of Goldberg-Shprintzen syndrome.

Axon outgrowth, degeneration, and KBP

Previous biochemical characterization showed that KBP binds to the closely related kinesin motor proteins Kif1B and Kif1C, and immunolocalization studies showed that it is associated with mitochondria (Wozniak et al., 2005). The same study showed that interfering with KBP function, either by overexpression of a deletion construct that disrupted the binding of KBP to Kif1B or by antisense knockdown of KBP, caused aggregation of mitochondria in cultured cells (Wozniak et al., 2005). Kif1Bα is one of two prominent nervous system isoforms of Kif1B and is thought to bind to mitochondria (Nangaku et al., 1994). In vitro motility assays suggested that KBP might increase the motility of Kif1Bα (Wozniak et al., 2005). Together, these data led to the hypothesis that the primary function of KBP may be to regulate mitochondrial transport by modulating the function of Kif1bα (Wozniak et al., 2005).

Disruption of mitochondrial transport and function has been associated with axonal degeneration (Coleman, 2005), a phenotype characteristic of *kbp* mutants. Blockade of mitochondrial transport is likely to decrease available ATP in the axon distal to the disruption of transport. This disrupts the function of the Na^+ K^+ ATPase, which causes a cascade of events that leads to an influx of Na^+ and Ca^{2+} ions into the axon and the subsequent activation of enzymes that lead to the degradation of the cytoskeleton, the formation of axonal swellings and ultimately axonal degeneration (Coleman, 2005). We frequently observed swollen mitochondria in mutant axons, particularly in the CNS, suggesting that it is possible that mitochondrial dysfunction leads to degeneration in the *kbp* mutant.

It is not clear, however, how a KBP-Kif1B mitochondrion-related function might regulate axonal outgrowth in vivo. Indeed, it has been shown that the main isoform of Kif1B that is expressed in the brain lacks the mitochondrial-binding domain (Conforti et al., 1999) and Kif1B mutant mice do not have defects in mitochondrial transport in axons (Zhao et al., 2001), suggesting that the role of Kif1B in regulating mitochondrial transport might be limited or fulfilled by another kinesin, such as Kif5B (Tanaka et al., 1998). Because KBP binds to the motor domain of Kif1B and Kif1C, and the motor domains of kinesin proteins are similar, it is possible that KBP is essential for the activity of yet other kinesins and thus the transport of other cargo.

KBP, microtubule organization and axonal development

Our analyses demonstrate that KBP has a key role in the regulation of microtubule organization. It is possible that the primary defect in *kbp* mutants is disorganization of microtubules, which would in turn cause secondary disruptions in the localization of axonal constituents. Supporting this possibility, disruption to microtubules is the first phenotype that we observed in our ultrastructural analyses of the *kbp* mutants. Similar disruptions in microtubules have not been described in mammalian *kif1* mutants, raising the possibility that KBP regulates microtubule dynamics independent of Kif1 kinesins. Axonal microtubules are regulated at many levels, and any of these could potentially involve KBP. For example, stathmin controls the availability of soluble tubulin molecules (Fletcher and Rorth, 2007); the tubulin specific chaperone e (tbce) ensures proper folding of α-tubulin and regulates tubulin heterodimer formation (Kortazar et al., 2007); SCG10 regulates the dynamics of microtubules in growing axons (Belmont and Mitchison, 1996; Riederer et al., 1997; Suh et al., 2004); and microtubule-associated proteins (MAPs), such as tau, have a number of important functions. In fact, *tbce* mutant mice have a somewhat similar phenotype to our *kbp* mutant, with disruption to axonal microtubules and subsequent axonal degeneration (Martin et al., 2002). Further biochemical studies will be required to elucidate the mechanisms by which KBP regulates the axonal cytoskeleton.

KBP and symptoms of GSS

Mutation of KBP (KIAA1279) causes Goldberg-Shprintzen syndrome in humans (Brooks et al., 2005). Though rare, GSS has very severe symptoms, for which there are currently no treatments. One of the most consistent features of this syndrome is disruption to white matter tracts (Ohnuma et al., 1997; Silengo et al., 2003). We believe that the zebrafish *kbp*^{st23} mutation provides a good model of these defects in myelinated axons. We suggest that the cellular basis of these myelinated axon symptoms in GSS is disruption to axonal microtubules. Our results also demonstrated that axons in the *kbp* mutant ENS are disrupted, suggesting that axonal abnormalities in the ENS may reveal a novel mechanism by which Hirschsprung's disease-like symptoms can emerge. Hirschsprung's is typically thought to be caused by defects in neural crest development (Amiel et al., 2000), whereas the first defects in the ENS of the *kbp*^{st23} mutant arise in differentiated neurons. Although we did not see an obvious reduction in the number of ENS neurons at the stages examined, it is possible that neurons are lost later, as a secondary consequence of initial disruption to axons. Indeed, in a mammalian model of Alzheimer's disease, disruption to axons was observed up to a year before the more commonly recognized disease-related neuronal pathology (Stokin et al., 2005).

Further analyses of our zebrafish *kbp* mutant may provide a basis to pursue and evaluate potential therapies for Goldberg-Shprintzen syndrome and axonal degeneration. The zebrafish is emerging as an ideal system in which to carry out drug discovery screens in vivo (Murphey and Zon, 2006; Peterson et al., 2004; North et al., 2007). Identification of compounds that affect KBP activity may provide mechanistic insight into its function that may not be easily derived from other approaches.

Conclusions

Our analysis demonstrates that *kbp* is required to organize the axonal cytoskeleton, regulate the speed of axonal outgrowth, localize axonal cargo and maintain the longer-term integrity of axons. These data show that *kbp* is required for multiple stages of axonal development and provide the first animal model of symptoms of Goldberg- Shprintzen syndrome.

We thank Joann Buchanan for excellent advice on the preparation of larvae and John Perrino for expert technical help with TEM. We thank Dominik Paquet for sharing the mito:mCherry construct. We are grateful to members of our laboratory for helpful discussions and comments on the manuscript. This work was supported by a National Institutes of Health (NIH) grant (NS050223, W.S.T.), an award from the Rita Allen Foundation (W.S.T.), a fellowship from Telethon Italy (GFP03011 to S.M.) and a postdoctoral fellowship from the Muscular Dystrophy Association (MDA4061, D.A.L.).

Supplementary material

Supplementary material for this article is available at
http://dev.biologists.org/cgi/content/full/135/3/599/DC1

References

Amiel, J., Salomon, R., Attie-Bitach, T., Touraine, R., Steffann, J., Pelet, A., Nihoul-Fekete, C., Vekemans, M., Munnich, A. and Lyonnet, S. (2000). [Molecular genetics of Hirschsprung disease: a model of multigenic neurocristopathy]. *J. Soc. Biol.* **194**, 125-128.

Baas, P. W. and Qiang, L. (2005). Neuronal microtubules: when the MAP is the roadblock. *Trends Cell Biol.* **15**, 183-187.

Belmont, L. D. and Mitchison, T. J. (1996). Identification of a protein that interacts with tubulin dimers and increases the catastrophe rate of microtubules. *Cell* **84**, 623-631.

Brooks, A. S., Breuning, M. H., Osinga, J., vd Smagt, J. J., Catsman, C. E., Buys, C. H., Meijers, C. and Hofstra, R. M. (1999). A consanguineous family with Hirschsprung disease, microcephaly, and mental retardation (Goldberg-Shprintzen syndrome). *J. Med. Genet.* **36**, 485-489.

Brooks, A. S., Bertoli-Avella, A. M., Burzynski, G. M., Breedveld, G. J., Osinga, J., Boven, L. G., Hurst, J. A., Mancini, G. M., Lequin, M. H., de Coo, R. F. et al. (2005). Homozygous nonsense mutations in KIAA1279 are associated with malformations of the central and enteric nervous systems. *Am. J. Hum. Genet.* **77**, 120-126.

Coleman, M. (2005). Axon degeneration mechanisms: commonality amid diversity. *Nat. Rev. Neurosci.* **6**, 889-898.

Conforti, L., Buckmaster, E. A., Tarlton, A., Brown, M. C., Lyon, M. F., Perry, V. H. and Coleman, M. P. (1999). The major brain isoform of kif1b lacks the putative mitochondria-binding domain. *Mamm. Genome* **10**, 617-622.

Duncan, J. E. and Goldstein, L. S. (2006). The genetics of axonal transport and axonal transport disorders. *PLoS Genet.* **2**, e124.

Fletcher, G. and Rorth, P. (2007). Drosophila stathmin is required to maintain tubulin pools. *Curr. Biol.* **17**, 1067-1071.

Fryer, A. E. (1998). Goldberg-Shprintzen syndrome: report of a new family and review of the literature. *Clin. Dysmorphol.* **7**, 97-101.

Gilmour, D. T., Maischein, H. M. and Nusslein-Volhard, C. (2002). Migration and function of a glial subtype in the vertebrate peripheral nervous system. *Neuron* **34**, 577-588.

Goldberg, R. B. and Shprintzen, R. J. (1981). Hirschsprung megacolon and cleft palate in two sibs. *J. Craniofac. Genet. Dev. Biol.* **1**, 185-189.

Gordon-Weeks, P. R. (2004). Microtubules and growth cone function. *J. Neurobiol.* **58**, 70-83.

Grenningloh, G., Soehrman, S., Bondallaz, P., Ruchti, E. and Cadas, H. (2004). Role of the microtubule destabilizing proteins SCG10 and stathmin in neuronal growth. *J. Neurobiol.* **58**, 60-69.

Hirokawa, N. and Takemura, R. (2005). Molecular motors and mechanisms of directional transport in neurons. *Nat. Rev. Neurosci.* **6**, 201-214.

Jontes, J. D., Buchanan, J. and Smith, S. J. (2000). Growth cone and dendrite dynamics in zebrafish embryos: early events in synaptogenesis imaged in vivo. *Nat. Neurosci.* **3**, 231-237.

Kortazar, D., Fanarraga, M. L., Carranza, G., Bellido, J., Villegas, J. C., Avila, J. and Zabala, J. C. (2007). Role of cofactors B (TBCB) and E (TBCE) in tubulin heterodimer dissociation. *Exp. Cell Res.* **313**, 425-436.

Mandelkow, E. M., Stamer, K., Vogel, R., Thies, E. and Mandelkow, E. (2003). Clogging of axons by tau, inhibition of axonal traffic and starvation of synapses. *Neurobiol. Aging* **24**, 1079-1085.

Maness, P. F. and Schachner, M. (2007). Neural recognition molecules of the immunoglobulin superfamily: signaling transducers of axon guidance and neuronal migration. *Nat. Neurosci.* **10**, 19-26.

Manna, T., Grenningloh, G., Miller, H. P. and Wilson, L. (2007). Stathmin family protein SCG10 differentially regulates the plus and minus end dynamics of microtubules at steady state in vitro: implications for its role in neurite outgrowth. *Biochemistry* **46**, 3543-3552.

Martin, N., Jaubert, J., Gounon, P., Salido, E., Haase, G., Szatanik, M. and Guenet, J. L. (2002). A missense mutation in Tbce causes progressive motor neuronopathy in mice. *Nat. Genet.* **32**, 443-447.

McHale, M. K., Hall, G. F. and Cohen, M. J. (1995). Early cytoskeletal changes following injury of giant spinal axons in the lamprey. *J. Comp. Neurol.* **353**, 25-37.

Meyer, M. P. and Smith, S. J. (2006). Evidence from in vivo imaging that synaptogenesis guides the growth and branching of axonal arbors by two distinct mechanisms. *J. Neurosci.* **26**, 3604-3614.

Murphey, R. D. and Zon, L. I. (2006). Small molecule screening in the zebrafish. *Methods* **39**, 255-261.

Murphy, H. R., Carver, M. J., Brooks, A. S., Kenny, S. E. and Ellis, I. H. (2006). Two brothers with Goldberg-Shprintzen syndrome. *Clin. Dysmorphol.* **15**, 165-169.

Nangaku, M., Sato-Yoshitake, R., Okada, Y., Noda, Y., Takemura, R., Yamazaki, H. and Hirokawa, N. (1994). KIF1B, a novel microtubule plus end-directed monomeric motor protein for transport of mitochondria. *Cell* **79**, 1209-1220.

North, T. E., Goessling, W., Walkley, C. R., Lengerke, C., Kopani, K. R., Lord, A. M., Weber, G. J., Bowman, T. V., Jang, I. H., Grosser, T. et al. (2007). Prostaglandin E2 regulates vertebrate haematopoietic stem cell homeostasis. *Nature* **447**, 1007-1011.

Ohnuma, K., Imaizumi, K., Masuno, M., Nakamura, M. and Kuroki, Y. (1997). Magnetic resonance imaging abnormalities of the brain in Goldberg-Shprintzen syndrome (Hirschsprung disease, microcephaly, and iris coloboma). *Am. J. Med. Genet.* **73**, 230-232.

Peterson, R. T., Shaw, S. Y., Peterson, T. A., Milan, D. J., Zhong, T. P., Schreiber, S. L., MacRae, C. A. and Fishman, M. C. (2004). Chemical suppression of a genetic mutation in a zebrafish model of aortic coarctation. *Nat. Biotechnol.* **22**, 595-599.

Pogoda, H. M., Sternheim, N., Lyons, D. A., Diamond, B., Hawkins, T. A., Woods, I. G., Bhatt, D. H., Franzini-Armstrong, C., Dominguez, C., Arana, N. et al. (2006). A genetic screen identifies genes essential for development of myelinated axons in zebrafish. *Dev. Biol.* **298**, 118-131.

Polleux, F., Ince-Dunn, G. and Ghosh, A. (2007). Transcriptional regulation of vertebrate axon guidance and synapse formation. *Nat. Rev. Neurosci.* **8**, 331-340.

Qiang, L., Yu, W., Andreadis, A., Luo, M. and Baas, P. W. (2006). Tau protects microtubules in the axon from severing by katanin. *J. Neurosci.* **26**, 3120-3129.

Riederer, B. M., Pellier, V., Antonsson, B., Di Paolo, G., Stimpson, S. A., Lutjens, R., Catsicas, S. and Grenningloh, G. (1997). Regulation of microtubule dynamics by the neuronal growth-associated protein SCG10. *Proc. Natl. Acad. Sci. USA* **94**, 741-745.
Sato, T., Takahoko, M. and Okamoto, H. (2006). HuC:Kaede, a useful tool to label neural morphologies in networks in vivo. *Genesis* **44**, 136-142.
Schilling, T. F., Piotrowski, T., Grandel, H., Brand, M., Heisenberg, C. P., Jiang, Y. J., Beuchle, D., Hammerschmidt, M., Kane, D. A., Mullins, M. C. et al. (1996). Jaw and branchial arch mutants in zebrafish I: branchial arches. *Development* **123**, 329-344.
Silengo, M., Ferrero, G. B., Tornetta, L., Cortese, M. G., Canavese, F., D'Alonzo, G. and Papalia, F. (2003). Pachygyria and cerebellar hypoplasia in Goldberg-Shprintzen syndrome. *Am. J. Med. Genet. A* **118**, 388-390.
Stamer, K., Vogel, R., Thies, E., Mandelkow, E. and Mandelkow, E. M. (2002). Tau blocks traffic of organelles, neurofilaments, and APP vesicles in neurons and enhances oxidative stress. *J. Cell Biol.* **156**, 1051-1063.
Stokin, G. B., Lillo, C., Falzone, T. L., Brusch, R. G., Rockenstein, E., Mount, S. L., Raman, R., Davies, P., Masliah, E., Williams, D. S. et al. (2005). Axonopathy and transport deficits early in the pathogenesis of Alzheimer's disease. *Science* **307**, 1282-1288.
Suh, L. H., Oster, S. F., Soehrman, S. S., Grenningloh, G. and Sretavan, D. W. (2004). L1/Laminin modulation of growth cone response to EphB triggers growth pauses and regulates the microtubule destabilizing protein SCG10. *J. Neurosci.* **24**, 1976-1986.
Talbot, W. S. and Schier, A. F. (1999). Positional cloning of mutated zebrafish genes. *Methods Cell Biol.* **60**, 259-286.
Tanaka, H., Ito, J., Cho, K. and Mikawa, M. (1993). Hirschsprung disease, unusual face, mental retardation, epilepsy, and congenital heart disease: Goldberg-Shprintzen syndrome. *Pediatr. Neurol.* **9**, 479-481.
Tanaka, Y., Kanai, Y., Okada, Y., Nonaka, S., Takeda, S., Harada, A. and Hirokawa, N. (1998). Targeted disruption of mouse conventional kinesin heavy chain, kif5B, results in abnormal perinuclear clustering of mitochondria. *Cell* **93**, 1147-1158.
Wozniak, M. J., Melzer, M., Dorner, C., Haring, H. U. and Lammers, R. (2005). The novel protein KBP regulates mitochondria localization by interaction with a kinesin-like protein. *BMC Cell Biol.* **6**, 35.
Yomo, A., Taira, T. and Kondo, I. (1991). Goldberg-Shprintzen syndrome: Hirschsprung disease, hypotonia, and ptosis in sibs. *Am. J. Med. Genet.* **41**, 188-191.
Yu, W., Solowska, J. M., Qiang, L., Karabay, A., Baird, D. and Baas, P. W. (2005). Regulation of microtubule severing by katanin subunits during neuronal development. *J. Neurosci.* **25**, 5573-5583.
Zhao, C., Takita, J., Tanaka, Y., Setou, M., Nakagawa, T., Takeda, S., Yang, H. W., Terada, S., Nakata, T., Takei, Y. et al. (2001). Charcot-Marie-Tooth disease type 2A caused by mutation in a microtubule motor KIF1Bbeta. *Cell* **105**, 587-597.
Zou, Y. and Lyuksyutova, A. I. (2007). Morphogens as conserved axon guidance cues. *Curr. Opin. Neurobiol.* **17**, 22-28.